Volume Title
ASP Conference Series, Vol. **Volume Number**
Author
© **Copyright Year** Astronomical Society of the Pacific

arXiv:1608.01556v1 [astro-ph.GA] 4 Aug 2016

FIR extended emission from cold gas and dust in Blue Compact Dwarf Galaxies: the anomalous cases of POX 186 and UM 461[1]

Vanessa Doublier[1], Aurélie Rémy-Ruyer[2] and SAG2 consortium

[1]*Max Planck for Extraterrestrische Physik, Giessenbachstr. 1, 85748 Garching, Germany*

[2]*Laboratoire AIM, CEA/IRFU/Service dAstrophysique Université Paris Diderot Bat. 709, 91191 Gif-sur-Yvette, France*

Abstract. FIR observation of BCD galaxies with Herschel has revealed a wealth of new insights in these objects which are thought to resemble high-redshift forming galaxies. Dust and cold gas showed to be colder, in more or less quantities than expected and of uncertain origin. However, not unlike in the local universe, not all the dust or the cold gas is accounted for, making it more challenging. SPICA and its factor 10 to 100 in sensitivity will allow to image the faint extended cold gas/dusty disks in BCDGs in addition to detect faint C and O lines only marginally or not at all detected by Herschel.

1. Two BCDGs out of norms

Blue Compact Dwarf Galaxies (BCDGs) are objects considered both as local analogs to high redshift early forming galaxies and as, paradoxically, left-overs from the cosmological history. Low metallicity, low dust content, relatively high star formation rates (wrt to total mass), large gas-to-star ratios, dwarf galaxies have been observed over two decades at all wavelengths to understand their evolution, how they survived the various cosmological events that punctuated the cosmological history. Recently combining high sensitivity and spatial resolution Herschel observations (covering at the wavelength range between 50μm and 500μm) with previous MIPS observations, it was shown that the dust properties as function of the star-formation rate and metallicity in low metallicity dwarf galaxies (12+log(O/H) < 8.1) behave very differently from higher metallicity dwarf galaxies and other normal galaxies.

UM 461 and POX 186 are two different BCDGs with almost opposite properties: UM 461 is a low metallicity gas rich with an underlying old stellar population (< 5 Gyrs) dwarf galaxy (figure 1 *Right*, (Lagos et al. 2011), (Doublier et al. 2001)) while POX 186 is a low metallicity gas poor with no apparent underlying old stellar population ultra compact dwarf galaxy (figure 1 *Left*, (Corbin & Vacca 2002)), (Doublier et al. 2000)).

[*] *Herschel* is an ESA space observatory with science instruments provided by European-led Principal Investigator consortia and with important participation from NASA.

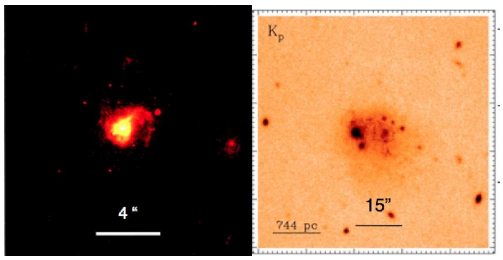

Figure 1. *Left:* POX 186: HST VRI *Right:* UM 461: K band

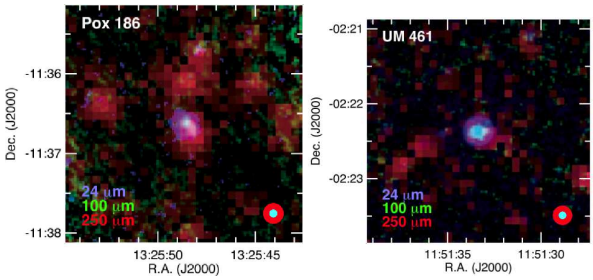

Figure 2. RGB composite image: 24μm MIPS and HERSCHEL Pacs 100μm +Spire 250μm *Left:* POX 186 *Right:* UM 461

2. Dust properties in POX 186 and UM 461

POX 186 and UM 461 (figure 2) were observed as part of the "Dwarf Galaxies Survey" (PI: S. Madden, (Madden et al. 2013)). For both objects the following data were obtained using the Herschel observatory with PACS: 70μm, 100μm and 160μm and SPIRE 250μm, 350μm and 500μm. The details of the data processing, photometry and spectral energy distribution fit is given in (Rémy-Ruyer et al. 2013) and Rémy-Ruyer et al. (2013 in prep). The MIPS data at 24μm were taken from (Bendo, Galliano, & Madden 2012).

2.1. SED

In the MIR + FIR, POX 186 does not show the same features as in the visible (Figure 2, *Left*). The galaxy displays a cold tail which origin is unclear: cold gas/dust tail/arm. POX 186 is an archetypical "dark galaxy".

POX 186 and UM 461 are is plotted on figure 3. Only upper limits could be obtained for POX 186 at 350μm and 500μm. This sets a lower limit for the dust and/or cold gas component temperatures. The blue symbols represent the fitted SED under the following assumptions: single dust component described by a modified Black-Body emission (see Rémy-Ruyer et al. (2013 in prep) for all details). The black line represents the modified BB models for the given dust mass, dust temperature and dust emissivity.

For POX 186, the observed SED appears to depart from the model at long wavelengths. The flat observed SED is indicative of very different components influencing

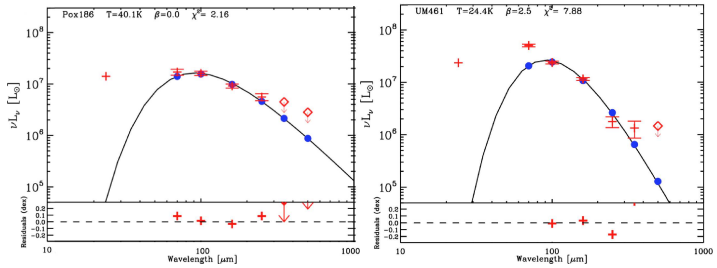

Figure 3. SEDs: Observed SED (red symbols), Fitted SED 1-component (blue symbols and black line), 2-component (yellow line) *Left:* POX 186 *Right* UM 461

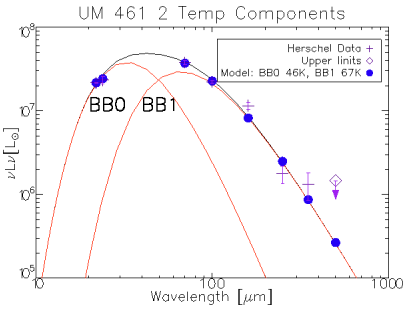

Figure 4. UM 461: 2-components modified BB SED

the energy distribution in the MIR and FIR. As seen in the two images: visible (figure 1 *Left*) and MIR+FIR (Figure 2, *Left*) there seems to be a warm component corresponding to the central star forming region, and much colder and extended underlying disk of gas/dust. However, the integrated photometry includes both regions and higher revolution with higher sensitivity would allow the disentangle the various components.

UM 461 shows two distinct components in the visible and near infrared which properties are different such as stellar population, star formation age and history. The Eastern star formation region shows much "younger" characteristics than the West star forming region (figure 2, *Right*). The distinctions are also reflected in the MIR+FIR range (figure 3, *Left*). One region (West) is much colder than the other (East).

The observed SED cannot be reproduced with a single dust component as shown in figure 3, *Right*. The fit diverges at both end of the energy distribution.

A second fit using a two-component modified black-body model was used and is shown in figure 4.

Contrary to POX 186, UM 461 shows the indication of hosting a warmer dust component possibly associated to the younger star formation located East. UM 461 could be a local counterpart of the high redshift SINSs galaxies inside which self- gravitating star forming regions temporarily form, then merge back into the galaxy disk.

2.2. Anomalous objects

In figure 5, the curves give theoretical Herschel flux ratios for simulated modified black bodies for β=[0.0, 2.5] and temperatures T=[0,40]K in 2K bins and T=[40,100]K in

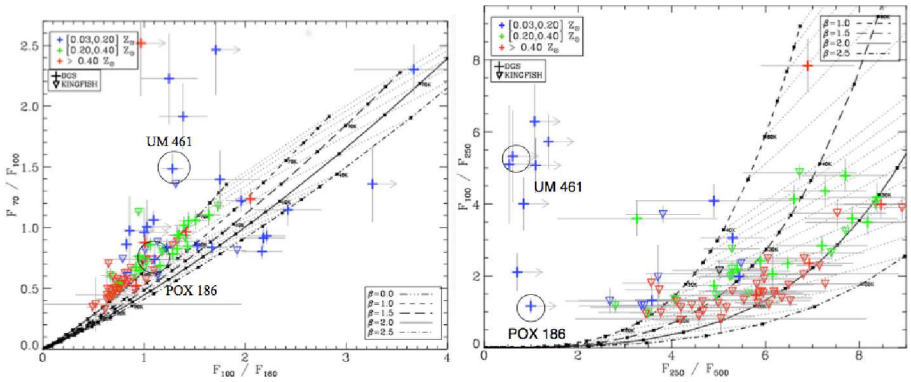

Figure 5. *Left* PACS/PACS diagram : F70/F100 versus F100/F160. the colours corresponds to different metallicity bins. Crosses and downward triangles represent DGS and KINGFISH galaxies, respectively. *Right* Colour-colour diagram : PACS/SPIRE diagram : F100 /F250 versus F250 /F500 .

10K bins (black dots). Lines of constant temperature are indicated as dotted lines (see Rémy-Ruyer et al. (2013 in prep)).

Note that POX 168 and UM 461 amongst the most metal poor galaxies (from 0.03 to 0.20 Z⊙) are very faint and even not detected anymore at longer wavelength. However, when detected their MIR properties differ from the bulk of dwarf galaxies. The dust composition, temperature and spatial distribution may be very different due to the very low metallicity and the particulars of the star formation event.

3. SAFARI

In coordination with interferometric submm-radio telescopes (Alma (in the southern hemisphere), Plateau de Bures) to cover the SED colder components at high spatial resolution, SPICA represents the perfect follow up tool for local BCDGs, and to search and study higher redshift (z~0.5 - 1) dwarfs. It will allow to spatially resolve both galaxies and structures and detect down to 210μm all components responsible for the anomalous SED shape and allow multiple components fitting

Acknowledgments. V. Doublier Pritchard wishes to thanks the SAG-2 consortium for allowing the use of GTO data, and A. Rémy-Ruyer for providing the SED and SED-fits of the 2 cases here discussed.

References

Bendo, G. J., Galliano, F., & Madden, S. C. 2012, MNRAS, 423, 197
Corbin, M. R., & Vacca, W. D. 2002, ApJ, 581, 1039
Doublier, V., Caulet, A., & Comte, G. 2001, A&A, 367, 33
Doublier, V., Kunth, D., Courbin, F., & Magain, P. 2000, A&A, 353, 887
Lagos, P., Telles, E., Nigoche-Netro, A., & Carrasco, E. R. 2011, AJ, 142, 162
Madden, S. C., Rémy-Ruyer, A., Galametz, M., Cormier, D., & et al. 2013, PASP, 125, 600
Rémy-Ruyer, A., Madden, S. C., Galliano, F., & et al. 2013, A&A, 557, A95